en
Experimental Neurobiology

Original Article

The Change in Circadian Rhythms in P301S Transgenic Mice is Linked to Variability in Hsp70-related Tau Disaggregation

Song Mi Han[1,2], Yu Jung Jang[1,2], Eun Young Kim[2,3] and Sun Ah Park[1,2,4*]

[1]*Lab for Neurodegenerative Dementia, Department of Anatomy, Ajou University School of Medicine, [2]Neuroscience Graduate Program, Department of Biomedical Sciences, Ajou University Graduate School of Medicine, [3]Department of Brain Science, Ajou University School of Medicine, [4]Department of Neurology, Ajou University School of Medicine, Suwon 16499, Korea*

Circadian disruption often involves a neurodegenerative disorder, such as Alzheimer's disease or frontotemporal dementia, which are characterized by intraneuronal tau accumulations. The altered sleep pattern and diurnal rhythms in these disorders are the results of tau pathology. The circadian disturbance in reverse is thought to develop and potentially aggravate the condition. However, the underlying mechanism is not fully understood. In this study, perturbed oscillations in *BMAL1*, the core clock gene, were observed in P301S tau transgenic mice. Tau fractionation analysis of the hippocampus revealed profound fluctuations in soluble and insoluble tau protein levels that were in opposite directions to each other according to zeitgeber time. Interestingly, a diurnal oscillation was detected in the heat shock 70 kDa protein 1A (Hsp70) chaperone that was in-phase with soluble tau but out-of-phase with insoluble tau. Tau protein levels decreased in the soluble and insoluble fractions when Hsp70 was overexpressed in HEK293T cells. Transfection of the *BMAL1* carrying vector was continual with the increase in Hsp70 expression and diminished tau protein levels, and it was effectively attenuated by the knockdown of Hsp70, suggesting that Bmal1 could modulate tau protein by Hsp70. Our results suggest that altered circadian oscillations affect tau status and solubility by modulating Hsp70 expression in an experimental model of tau pathology. These findings suggest Hsp70 as a possible pathogenic link between circadian disruption and aggravations of tau pathology.

Key words: Tauopathies, Tau protein, Hsp70 heat-shock proteins, Circadian rhythm

INTRODUCTION

The accumulation of tau protein is observed in various neurodegenerative disorders, including Alzheimer's disease (AD) and frontotemporal dementia (FTD), which are referred to as tauopathies. Tau protein is a microtubule-binding protein and plays an important physiological role in neuronal cells, including the stabilization of microtubules [1], regulation of microtubule dynamics, axonal transport [2, 3], and prevention of DNA damage [4]. However, in pathological conditions tau protein is detached from microtubules, missorted into the somatodendritic portion, and self-aggregated, leading to various physiological functions loss and neurotoxicity [5, 6].

Circadian rhythms are a fundamental component of physiology, indicating 24-hour oscillations of biological processes in organisms [7]. Circadian dysregulations have been identified in AD, FTD, and other neurodegenerative disorders [8]. From the very early stage of AD, instability in circadian rhythms reveals deficient slow-wave activity during the deep-sleep stage, and it seems to be strongly associated with tau pathology on tau-PET and tau levels in cerebrospinal fluid [9]. A recent postmortem study demonstrated an increased number of tau-positive and pTau-positive neurons in the subcortical wake-promoting area was significantly correlated with the disturbances in sleep variables in AD patients [10]. Similar results have been reported in the animal model, P301S tau transgenic mice presenting tau pathology. More tau-

positive neurons were found in sleep-regulating brainstem regions in parallel with the depletion of the total quantity of sleep and slow-wave activity during sleep [11]. The extension of tau pathology and neurodegeneration into the core circadian regions like the suprachiasmatic nucleus and its connecting regions, including the hypothalamus and brainstem, is regarded as a primary mechanism of circadian dysregulation in tauopathies [10, 12]. In the viewpoint that circadian oscillation affects many brain functions and the impairment of the sleep-wake cycle increases the risk of neurodegenerative disease [13], the scenario in a reverse direction, circadian disruption gives an impact on tauopathies, is also possible. Therefore, it seems that circadian dysregulation and tau pathology have a feedforward interaction. Despite the observations supporting an intimate relationship between these fewer efforts have been paid to elucidate the precise mechanism.

The diurnal rhythms are controlled by transcription-translation feedback loops that show an oscillation with a 24-hour cycle. The positive loop is composed of a dimer of the brain and muscle ARNT- like 1 (Bmal1) and circadian locomotor output cycles protein kaput (Clock) that increases the transcriptions of enhancer boxes (E-box)-containing downstream targets, including period circadian protein homolog (Per) and cytochrome (Cry) protein [13]. When Per and Cry have increased in the cytoplasm, these bind to each other, move into the nucleus, and repress the Bmal1-Clock activity, eventually acting as a negative feedback loop [14]. The diurnal rhythm regulates clearing tau from the extracellular space and cerebrospinal fluid [15]. This may occur through modulation of the lymphatic system, the primary mechanism to clear extracellular solutes that is active during sleep [16, 17]. However, the clear evidence linking tau pathology and diurnal dysregulation demonstrated in tau mice and AD patients cannot be fully explained by the impact of circadian abnormality on the glymphatic system. As tau pathology are profound in intracellular compartments in patients with AD and related disorders, circadian misalignment could affect tau pathology through mechanism occurring at the cellular levels. Intracellular tau aggregates are cleared by the ubiquitin-proteasome system (UPS) and the autophagy-lysosomal system (ALS) depending on the size and the solubility. The soluble tau protein with low molecular weight is accessible to UPS while large and aggregated tau is mainly cleared by ALS [18]. Chaperone-mediated autophagy (CMA), although it has been less attentive regarding tau clearance, was shown to be involved in tau clearance [19]. The impairment of the clearance machinery is a prominent and common finding in neurodegenerative disorders, and the strategy to improve it is expected as a promising future treatment [19, 20]. In this study, we examined P301S tau transgenic mice at the age of 40~53 weeks that presented full-blown tau

pathology [21] to understand the molecular mechanism relating between circadian oscillations and tau pathology focusing on intracellular clearance events. The oscillations in the core circadian clock and the quantity of tau protein according to its solubility were examined with consideration of a 6 h-interval of zeitgeber time (ZT) in the appropriate brain subregions.

MATERIALS AND METHODS

Chemicals and antibodies

Chloroquine (CQ), MG132, and forskolin were obtained from Sigma-Aldrich (St. Louis, MO, USA). Primary antibodies for the corresponding proteins were obtained as follows: phosphorylated tau at threonine 231 (pT231) (Invitrogen, Waltham, MA, USA), total tau (A0024; Dako, Santa Clara, CA, USA), Bmal1 (Abcam, Cambridge, UK), Per2 (Alpha Diagnostic Intl. Inc., San Antonio, TX, USA), Hsp70 (Enzo Life Sciences, Farmingdale, NY, USA), vinculin (Sigma-Aldrich), and ubiquitin and glyceraldehyde 3-phosphate dehydrogenase (GAPDH) (Santa Cruz Biotechnology, Dallas, TX, USA). Secondary antibodies for immunoblot or immunofluorescence included horseradish peroxidase-conjugated rabbit and mouse IgG from Molecular Probes (Eugene, OR, USA), anti-rabbit or anti-mouse Alexa Fluor 488 and 555 from Invitrogen.

Constructs

pEGFP-C1–4R tau was provided by Dr. Kenneth S. Kosik [22]. We purchased the pcDNA 3.1 vector, pEGFP-C3, pEGFP-Hsp70 (addgene, Watertown, MA, USA), pCDH-CMV-MCS-t2A-copGFP (#CD524A-1, System Biosciences, Palo Alto, CA, USA), and pCDH-EF1-MCS-T2A-Puro (Biocat GmbH, Heidelberg, Germany). pCMV-HA-Bmal1 was cloned using XhoI and NotI (NEB, Ipswich, MA, USA). Bmal1 was amplified using the polymerase chain reaction (PCR) from the 5'-end methionine (XhoI site) to the 3'-end stop codon (NotI site) out of cDNA from NIH 3T3 cells.

To generate pCDH-CMV-MCS-T2A-Puro, the copGFP region of pCDH-CMV-MCS-t2A-copGFP was changed to puromycin from pCDH-EF1-MCS-T2A-Puro using NotI and SalI. 4R tau was amplified using PCR from the 5'-end methionine (EcoRI site) to the 3'-end stop codon (BamHI site) using the pEGFP-C1–4R tau vector, and it was cloned to pCDH-CMV-MCS-T2A-Puro using the EcoRI and BamHI restriction enzymes (NEB). Furthermore, the 4R tau (P301S) mutant construct was generated to obtain pCDH-CMV-4R tau (P301S)-T2A-Puro using a site-directed mutagenesis kit (Agilent Technologies, Santa Clara, CA, USA).

The short hairpin RNA (shRNA) plasmid was generated using

pLKO.3G_X7 plasmid (Addgene, #171213). To anneal the DNA strands, two single-strand DNAs were co-incubated at 95℃ for 4 min, at 70℃ for 10 min, and then slowly cooled down to room temperature for five hours using a ProFlex PCR System (Enzo Life Sciences). pLKO.3G_X7 plasmid was digested using AgeI and EcoRI at 37℃ for 2 h and purified using NucleoSpin Gel and PCR Clean-up kit (Macherey-Nagel, Dueren, Germany). Ligation of 4 μl annealed oligo and 1 μl digested pLKO.3G_X7 plasmid was performed using T4 ligase at 20℃ for 16 h. The sequences of shRNA targeting Hsp70 were described below; sense strand: 5'-CCGGCCAATCGAGAATCAGCTATTACTCGAGTA-ATAGCTGATTCTCGATTGGTTTTTTG-3', antisense strand: 5'-AATTCAAAAAACCAATCGAGAATCAGCTATTACTC-GAGTAATAGCTGATTCTCGATTGG-3'.

Animals

Wild-type and P301S tau transgenic mice were purchased from the Jackson Laboratory (PS-19, stock #008169, Sacramento, CA, USA). The animals were maintained under a 12-h light-dark cycle (lights on from 7:00 a.m. to 7:00 p.m.) in standard animal cages and were provided with free access to food and water. The animals were maintained in a specific pathogen-free laboratory at the animal research center of Ajou University Medical Center. All animal experiments were approved by the animal research committee of the institution (IACUC protocol 2021-0025). The wild-type or P301S mice (40~53 weeks of age, male, *n*=3 per group) were killed every 6 h during a 24 h cycle at ZT2, ZT8, ZT14, and ZT20 for the mRNA, protein, and immunohistochemistry analyses. ZT was determined according to the light-dark cycles (12:12 h) whereby the lights were on at ZT0.

Cell culture

HEK293T cells were purchased from the American Type Culture Collection (ATCC, Manassas, VA, USA). The cells were cultured in high glucose DMEM (WELGENE Inc., Daegu, Republic of Korea), supplemented with 10% fetal bovine serum and 1% penicillin/streptomycin (GIBCO-BRL, Grand Island, NY, USA) in 5% CO_2 at 37℃.

Transfection

The cells were seeded at 1.5×10^5 cells in a 6-well plate. When they reached 50~60% confluence, the cells were transfected with the indicated constructs using Lipofectamine 2000 (Invitrogen) according to the manufacturer's instructions. The transfected cells were incubated for 24 h and treated with 10 μM forskolin for 24 h. To identify the tau degradation pathways, the cells were treated with 5 μM CQ and 2.5 μM MG132 for the last 12 h followed by protein

fractionation.

Tissue and cell sample preparation

The mouse brains were separately collected as the cortex, hippocampus, and diencephalon (including the hypothalamus and suprachiasmatic nucleus [SCN]) and post-fixed in 4% paraformaldehyde and cryoprotected in 30% sucrose solution. The tissues were frozen in isopentane and stored at -80℃ for later immunohistochemistry analysis. The tissues for the immunoblot assay were stored immediately at -80℃ until analysis.

The tissues were lysed in tris-buffered saline (TBS) solution containing a phosphatase and proteinase inhibitor cocktail (Roche, Basel, Switzerland) and incubated for 30 min on ice. Then, the lysates were centrifuged at 100,000×g for 1 h at 4℃. The supernatant was kept as the TBS fraction. The pellet was dissolved in radioimmunoprecipitation (RIPA) solution (150 mM NaCl, 1% NP-40, 0.5% sodium deoxycholate, 0.1% sodium dodecyl sulfate [SDS], 50 mM Tris [pH 8.0])) and subjected to the same conditions as before. The supernatant was kept as the RIPA fraction after adding the phosphatase and proteinase inhibitor cocktail. The pellet as the formic acid fraction was solubilized in 70% formic acid. Following 1 h incubation at room temperature, the lysate was centrifuged at 100,000×g for 30 min at 4℃. The supernatant was collected in buffer, which was changed to phosphate-buffered saline (PBS) using Amicon Ultra-0.5 Centrifugal Filter Unit (Millipore, Billerica, MA, USA). The sample was boiled with SDS sample buffer.

The cells were washed once in PBS and harvested in lysis buffer (150 mM NaCl and 50 mM Tris) containing 1% Triton X-100 and the phosphatase and proteinase inhibitor cocktail. The lysates were incubated on ice for 15 min and then centrifuged at 100,000×g for 30 min at 4℃. The supernatant was collected as the soluble fraction (Triton-X soluble fraction), and the pellet was resuspended in lysis buffer containing a 1% sarkosyl and the phosphatase and proteinase inhibitor cocktail, and incubated for 1 h (Triton-X insoluble fraction). After sonication, the lysate was centrifuged at 100,000×g for 30 min at 4℃. The pellet was resuspended in SDS sample buffer as the insoluble fraction and boiled at 95℃ for 15 min.

Immunoblot analysis

Samples containing equal quantities of protein were resolved by 6~10% sodium dodecyl sulfate-polyacrylamide gel electrophoresis and transferred to a polyvinylidene fluoride membrane (Millipore). The membrane was blocked with 5% bovine serum albumin (BSA) and incubated with primary antibodies overnight. After washing with PBS containing Tween-20, the membranes were subsequently incubated with peroxidase-conjugated secondary antibodies for

1 h. Protein bands incubated with enhanced chemiluminescence reagents (Advansta Inc., San Jose, CA, USA) were visualized using the iBright imaging system (Invitrogen).

Immunohistochemistry

The tissues were sliced into 18 μm free-floating sections. The tissue sections were washed three times in PBS to remove the stock solution (glycerol 30%, ethylene glycol 30%, 0.2 M PB buffer 10%; pH 7.2). Following the PBS washes, the tissues were permeabilized in 0.2% Triton X-100 in PBS (PBST) for 30 min. After blocking in 5% donkey serum for 1 h, the tissues were incubated overnight at 4℃ in primary antibodies (Per2 and Bmal1). After a wash in PBST, the tissues were incubated with secondary antibodies for 2 h at room temperature. The slides were mounted with Fluoromount-G (Southern Biotech, Birmingham, AL, USA) and visualized with the K1-Fluo confocal laser scanning microscope (Nanoscope Systems, Daejeon, Republic of Korea). The region of interest (ROI) was drawn along the SCN outline. The positive area (%) in the ROI was measured using ImageJ software (National Institutes of Health, Bethesda, Maryland, USA).

Immunocytochemistry

The cells were transfected with P301S and/or Hsp70 and fixed with 4% paraformaldehyde for 20 min at room temperature. Fixed cells were permeabilized with 0.2% PBST for 5 min and blocked in 5% BSA for 30 min. The cells were subsequently incubated with the indicated primary antibodies that were diluted in 5% BSA, washed three times, and further reacted with the secondary antibodies (anti-rabbit Alexa Fluor 555 and anti-mouse Alexa Fluor 488). Slides were mounted with Fluoromount-G and visualized with the confocal laser scanning microscope.

Reverse transcription-polymerase chain reaction (RT-PCR)

Total RNA was extracted from each brain region of the wild-type and P301S mice using an RNA isolation kit (Macherey-Nagel, Dueren, Germany). cDNA was synthesized using a cDNA synthesis kit (Enzynomics, Daejeon, Republic of Korea). Quantitative (q) RT-PCR was performed using the Bio-Rad Real-Time PCR System (Bio-Rad Laboratories Inc., Richmond, CA, USA). The forward (F) and reverse (R) primers used for the qPCR were *Per2* F, 5'-CAGACGCGCGGGGTTGA-3'; *Per2* R, 5'-CCGTGGAG-CAGTTCTCGTT-3'; *Bmal1* F, 5'-AGGCCTTCAGTAAAGGTG-GAA-3'; *Bmal1* R, 5'-GGTGGCCAGCTTTTCAAATA-3'; *Tbp* F, 5'-GGGAGAATCATGGACCAGAA-3'; *Tbp* R, 5'-CCGTA-AGGCATCATTGGACT-3'; *HSP70* F, 5'-ACCTACTCCGA-CAACCAA-3'; *HSP70* R, 5'-AGATGACCTCTTGACACTTG-3'; *TAU* F, 5'-ACTCTGCTCCAAGACCAAGAA-3'; *TAU* R, 5'-

TCTCCGATGCCTGCTTCT-3'; *GAPDH* F, 5'- GAAGGT-GAAGGTCGGAGT- 3'; *GAPDH* R, 5'- GAAGATGGT-GATGGGATTTC-3'.

Statistical analysis

All statistical analyses were performed using GraphPad Prism software 9.0 (GraphPad Software, Inc., San Diego, CA, USA). Differences were detected with the Mann-Whitney test or the Kruskal-Wallis test, followed by the Dunn post-hoc method. A p-value <0.05 was considered significant for all tests.

RESULTS

Disrupted circadian rhythms in the P301S tau transgenic mice

The expression of key circadian genes was first examined by immunohistochemistry in the brain sections containing the SCN where the master clock is located [23]. The peak Bmal1 expression in SCN was noted at ZT20 in the P301S mice, while it occurred at ZT8 in the wild-type mice (Fig. 1A). The diurnal changes in Per2 immunoreactivities were comparable between P301S and the wild-type mice, commonly peaking at ZT14. Next, we evaluated the transcript levels of Bmal1 and Per2 by qPCR using mRNA extracts from the diencephalon containing the SCN (Fig. 1B). The circadian oscillation of mRNA levels of Bmal1 was symmetric with those of Per2 according to ZT in wild-type mice. The lowest point of Bmal1 was the highest time for Per2. The inverse pattern of the oscillations of Bmal1 and Per2 shows their physiological feedback relationship. However, the typical relationship seemed to be lost in the tau transgenic mice: Bmal1 demonstrated an in-phase oscillation with Per2 peaking at ZT14. It showed decoupled circadian oscillations in the Bmal1 of P301S mice in comparison with the wild-type mice.

Next, we evaluated whether the aberrance in circadian oscillations was present in other brain areas. The cortex and hippocampus were harvested as a separate because these regions predominantly reveal tau pathology in P301S mice [24]. We found that the ZT-dependent transcript levels in Bmal1 and Per2 were not different between the wild-type and P301S mice in the cortex (Fig. 2A, *left*). However, the sequential changes of Bmal1 protein demonstrated a difference between P301S and the wild-type mice, revealing the lowest while the highest at the same ZT point (ZT20) respectively (Fig. 2A, *right*). In the case of Per2 protein, the quantity increased slightly in P301S but kept on a downhill in wild-type mice at ZT14, however, the overall oscillation pattern was similar between the two groups(Fig. 2A, *right*), The inconsistency in the circadian pattern of Bmal1 was more evident in the hippocampus
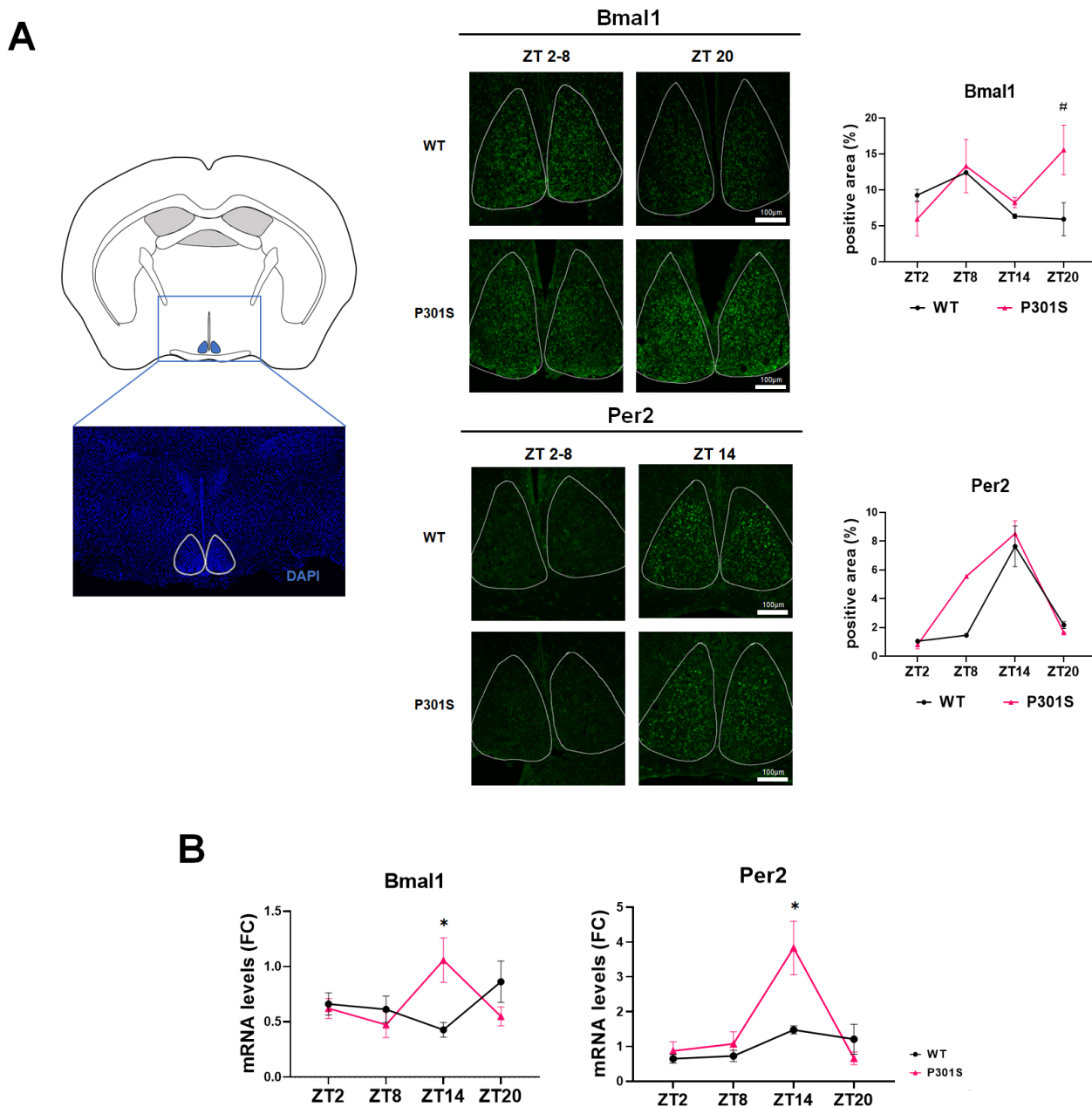
Fig. 1. Circadian expression of the master clock molecules in the suprachiasmatic nucleus. (A) The region of interest to examine the immunoreactivities of respective proteins in the suprachiasmatic nucleus is shown as a white lining on the brain section stained using 4′,6-diamidino-2-phenylindole (DAPI) (left). The representative photos of immunohistochemistry using Bmal1 (upper) and Per2 (lower) antibodies are shown according to the zeitgeber time (ZT) in wild-type (WT) and P301S mice (middle). The image analysis of diurnal changes of Bmal1 and Per2 immunoreactivities shows a significant difference at ZT20 in Bmal1 in wild-type vs. P301S tau mice (right). Scale bars, 100 μm. (B) The quantitative reverse transcription (qRT)-PCR data reveal a discrepancy between wild-type and P301S mice in the ZT-dependent level changes of Bmal1 and Per2 transcripts. Data are mean±SEM (n=3). *$p < 0.05$ and #$p < 0.1$ on Mann-Whitney test.

(Fig. 2B). The oscillations of mRNA and protein levels in reference to ZT were trivial in P301S mice, which was in contrast to those in wild-type mice. It made the discrepancy between be remarkable at ZT8 and ZT20. The mRNA level of Per2 was lower at ZT2 and ZT20 in P301S mice, but the protein levels remained comparable to those of wild-type mice. Our results suggest that the perturbation of oscillation patterns of Bmal1 had spread into other brain regions, particularly the hippocampus of P301S mice.
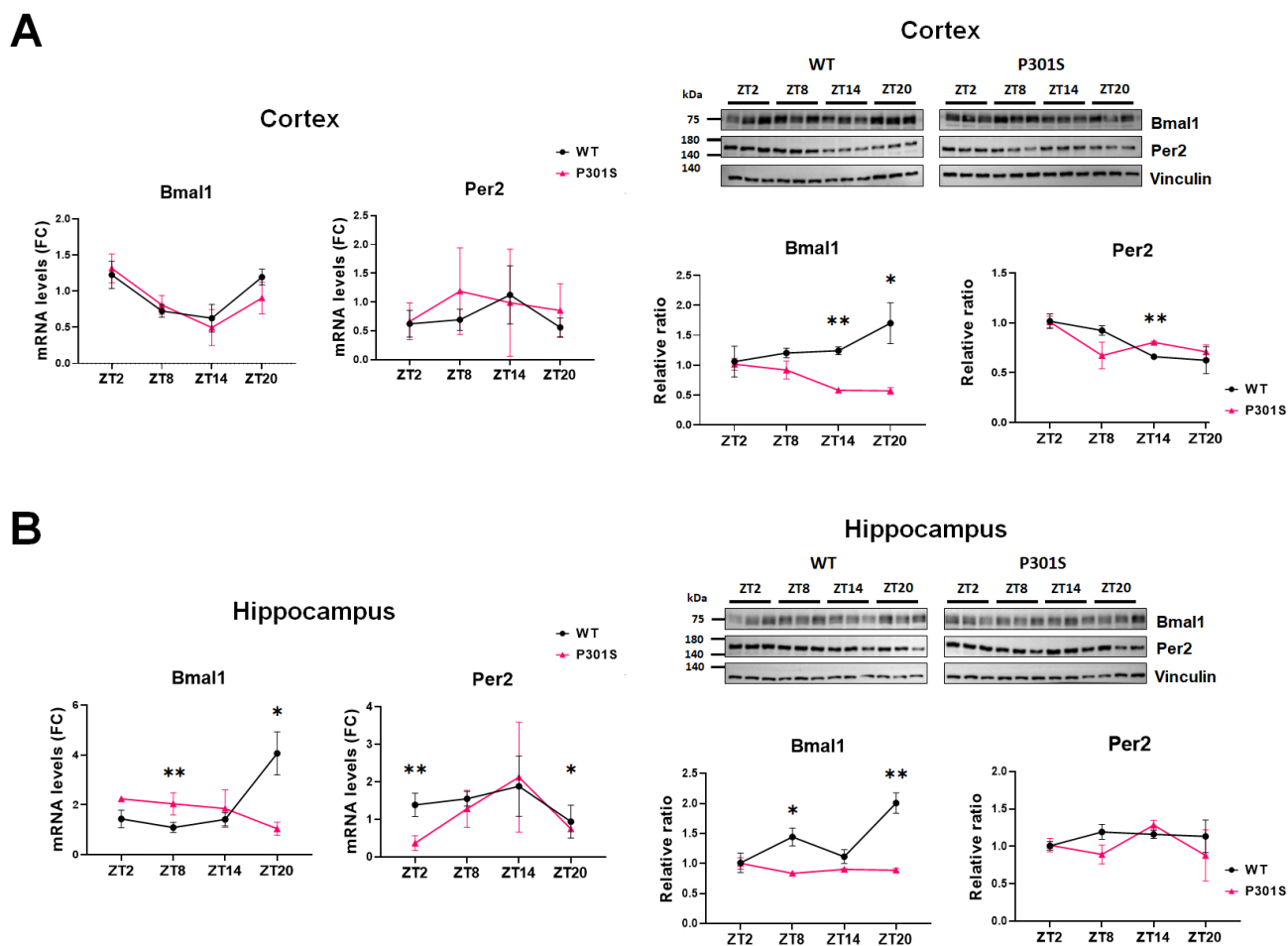
Fig. 2. The analysis of circadian oscillations of Bmal1 and Per2 in the cortex and the hippocampus. (A) The qRT-PCR (left) and western blot (right) of the cortex demonstrate a comparable pattern of mRNA oscillations in Bmal1 and Per2 between wild-type and P301S mice. The altered expression of Bmal1 protein is noted at ZT14 and ZT20 compared with the wild-type. (B) The qRT-PCR (left) and western blot (right) of the hippocampus reveals a disruption in circadian oscillations of Bmal1 in both transcript and protein levels in P301S mice. The mRNA level of Per2 was lower at ZT2 and ZT20 in P301S than in wild-type mice, but its overall pattern of oscillations and the protein levels are similar to those of wild-type mice. (A, B) Data are mean±SEM (n=3). Differences were detected with the Mann-Whitney test. *p<0.05, **p<0.01.

Oscillations in tau solubility relevant to the Hsp70 protein chaperone

We further investigated whether tau expression or its solubility was modulated according to the ZT points in the hippocampus. The serial extraction was performed to analyze the tau solubility and aggregations status [25]. The soluble tau in the TBS fraction that was extracted without the detergent showed a higher level at ZT20 than at ZT8 in P301S mice, but the phosphorylated tau at Thr 231 (pT231) did not reveal a significant expression change throughout the examined ZT points. Profound oscillations of pTau231 and tTau levels in P301S mice were notable on the western blot using RIPA-soluble fraction that contains less soluble proteins, which peaked at ZT14 (Fig. 3A). The ZT-related level changes were also distinct in the RIPA-insoluble, and formic acid

extractable fractions in which there are strongly aggregated forms such as tau in neurofibrillary tangles. The densitometry analysis of the western blot revealed that the direction of diurnal variability was symmetrical between the two fractions, as the highest in the RIPA-soluble fraction matched the lowest time-point of the RIPA-insoluble fraction (Fig. 3A). This finding suggests that the status of tau is modulated by the circadian clock. Recently, Hsp70 was reported to play a crucial role in the disassembly of tau fibrils into smaller species *in vitro* [26]. In addition, the transcription factor of Hsp70 is affected by Bmal1 when the circadian rhythm is impaired by UV irradiation in cultured cells [27]. These findings inspired us to explore the involvement of Hsp70 in tau fluctuations with special consideration given to tau solubility. The diurnal variability of Hsp70 in P301S mice differed from that in the wild-
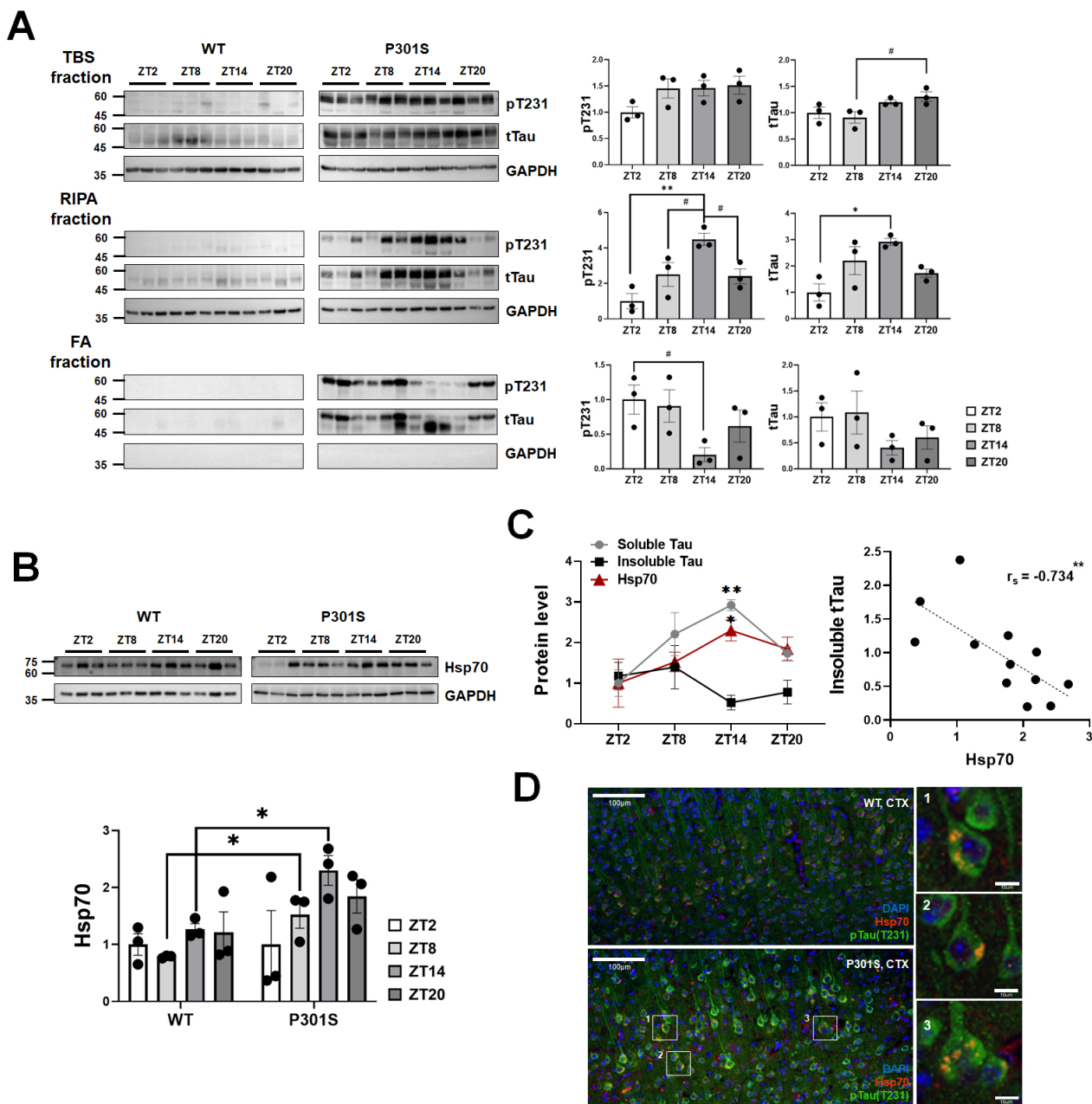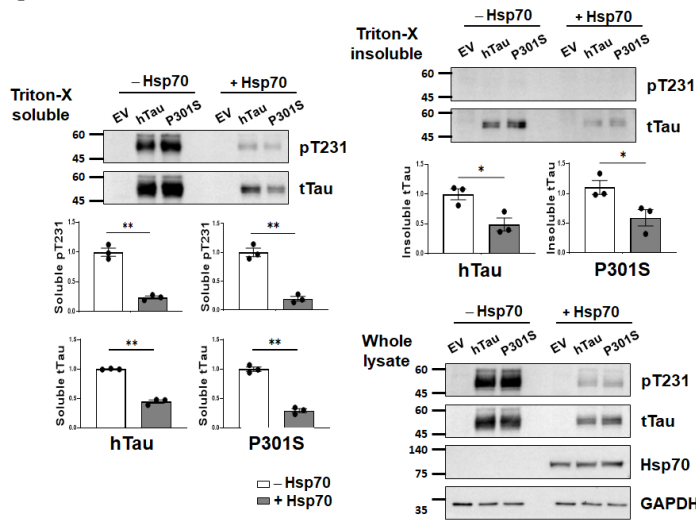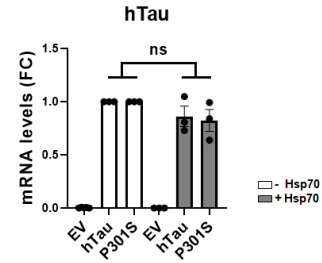
Fig. 3. Diurnal oscillations in tau protein solubility in relation to the expression of Hsp70 in the hippocampus of P301S transgenic mice. (A) The western blot using the serially extracted protein extracts and its densitometry analysis shows the circadian alterations of tau protein levels, both phosphorylated- and total tau, showing a specified pattern according to the status of tau solubility. ZT14 is specifically identified as the highest ZT point for the RIPA-soluble tau levels while the lowest time-point for the RIPA-insoluble tau protein at the same time. Data are mean±SEM (n=3). #p<0.1, *p<0.05 and, **p<0.01 on Kruskal-Wallis test adjusted for multiple comparisons using Dunn's post-hoc correction. (B) The ZT-associated alterations in Hsp70 protein expression in P301S mice are shown on western blot and densitometry analysis in comparison to wild-type mice. Data are mean±SEM (n=3). *p<0.05 on Kruskal-Wallis test followed by Dunn's post-hoc correction. (C) The circadian variability in Hsp70 protein levels is a similar pattern to that of the RIPA-soluble tau, but an opposite pattern to the RIPA-insoluble fraction suggesting the possible role of Hsp70 in tau disaggregation (left). The highest difference is noted at ZT14. Data are mean±SEM (n =3). *p<0.05 and **p<0.01 on Kruskal-Wallis test followed by Dunn's post-hoc correction. Spearman's correlation analysis (right) shows the negative correlation between Hsp70 and tau (rs=-0.7343, p<0.01). (D) Immunohistochemistry of cortical brain sections indicates co-localization of Hsp70 with tau proteins. Scale bars are 100 μm or 10 μm as indicated. CTX, cortex; FA, formic acid.
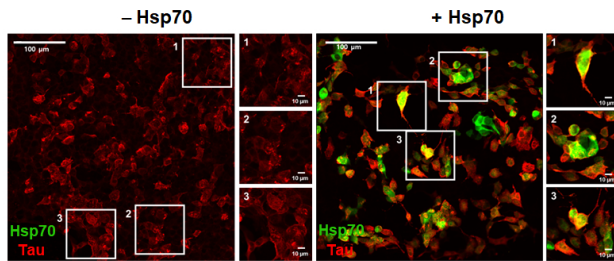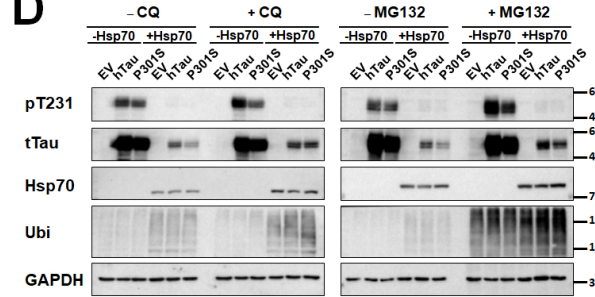
Fig. 4. The analysis of tau protein under the modulation of Hsp70 *in vitro*. (A) Markedly reduced tau protein levels both in phosphorylated- and total form are clearly noted after the co-expression of Hsp70 in all tested fractions, soluble, insoluble and whole fractions. Data are mean±SEM (n=3). *p<0.05 and **p<0.01 on Mann-Whitney test. (B) The mRNA levels of tau are not affected by Hsp70 co-expression. Data are mean±SEM (n=3). The 'ns' means that the comparison was insignificant at the level of p<0.05 on Mann-Whitney test. (C) The representative photos of immunocytochemistry for Hsp70 (green) and tau (red) show nice co-localizations under the overexpression of Hsp70 (right). Scale bars are 100 μm or 10 μm as indicated. (D) The western blots show a level change of the indicated proteins according to the ZT after the application of CQ (left) and MG132 (right). The decreased total tau proteins by Hsp70 overexpression are partly reversed by CQ and MG 132 treatment. EV, empty vector; FC, fold-change; ns, non-significance.

type mice, as expression increased at ZT8 with a peak at ZT14 (Fig. 3B). Interestingly, the pattern was in-phase with the RIPA-soluble tau fraction but out-of-phase with the RIPA-insoluble tau fraction (Fig. 3C). A negative correlation was confirmed between insoluble tau and the Hsp70 level (r_s=-0.734, p<0.01). In addition, Hsp70 was co-localized with tau in the neurons of P301S mice according to immunohistochemistry (Fig. 3D). These results support the possible contribution of Hsp70 toward reducing tau aggregations.

Involvement of Hsp70 in the modulation of tau clearance in vitro

To test the functional significance of Hsp70 in the regulation of tau proteins, Hsp70 was overexpressed in HEK293T cells with or without additional expression of human tau, either wild-type or P301 mutant tau. We treated the cells with forskolin (10 μM)

to accelerate tau aggregation [28]. Tau protein levels, both phosphorylated- and total tau in the soluble and insoluble fractions decreased after overexpressing Hsp70 (Fig. 4A), but the mRNA level was not altered by it (Fig. 4B), which indicates that Hsp70 is mainly involved in tau degradation. When we performed the immunocytochemistry of Hsp70 and tau, Hsp70 was found to co-localize with tau protein (Fig. 4C). Subsequently, we examined the functional involvement of autophagy and proteasome in tau degradation by Hsp70. The autophagy inhibitor CQ as well as the proteasome inhibitor MG132 effectively attenuated tau degradation by Hsp70 (Fig. 4D). These results suggest that Hsp70 regulates tau degradation in an autophagy-dependent and proteasome-dependent manner.
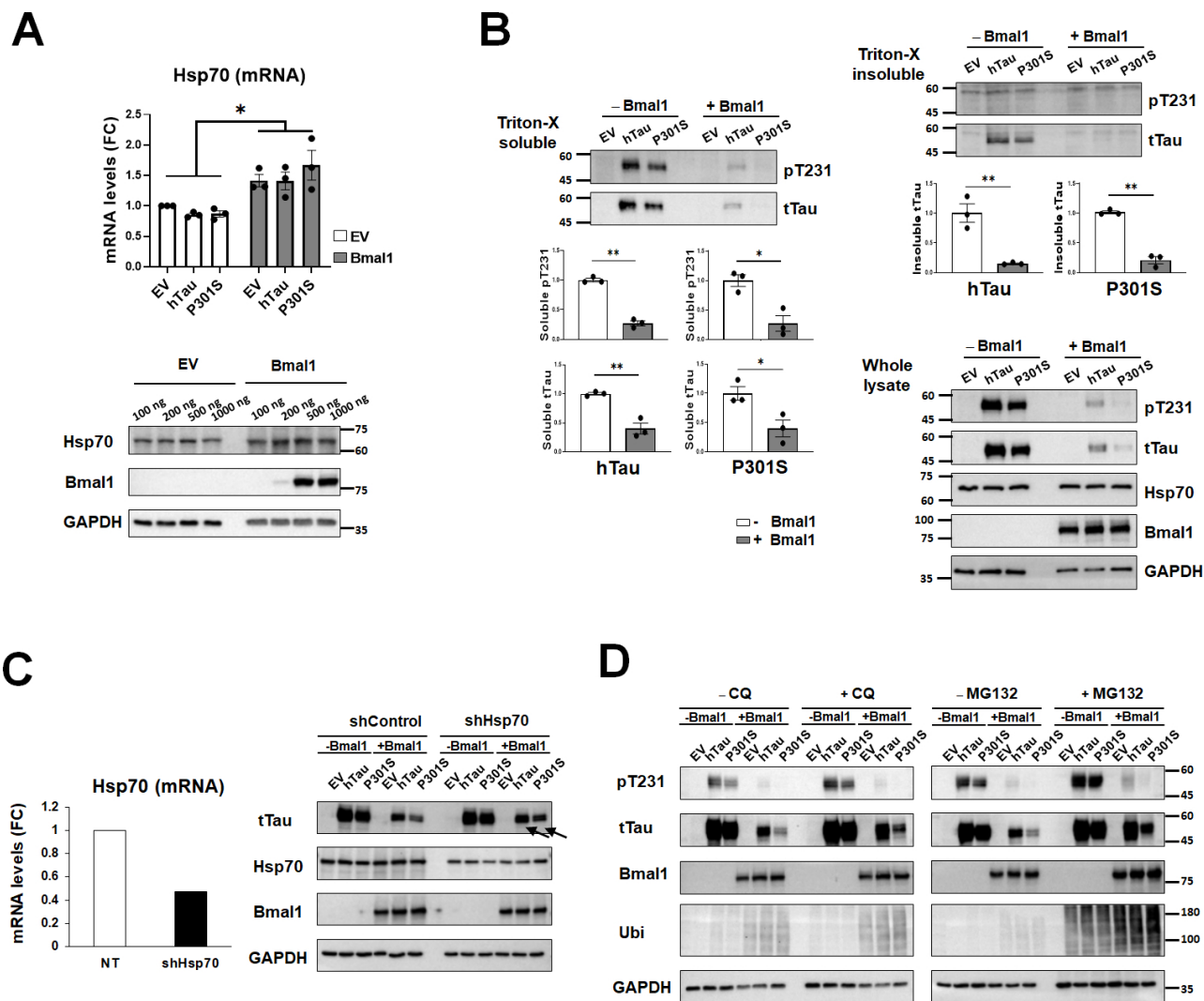
Fig. 5. The analysis of tau protein under the modulation of Bmal1 *in vitro*. (A) The qRT-PCR (upper) and western blot (lower) data show that Bmal1 overexpression increases the mRNA and protein levels of Hsp70 in HEK293T cells. Data are shown in mean±SEM (n=3). *p<0.05 on Mann-Whitney test. (B) The marked reduction of tau levels is noted in all tested fractions after Bmal1 overexpression. Data are mean±SEM (n=3). *p<0.05 and **p<0.01. (C) The transfection of the short-hairpin RNA vector for Hsp70 (shHsp70) effectively diminishes the transcription (left) and protein expression (right) of Hsp70. The diminution of tau protein levels by Bmal1 overexpression is attenuated by shHsp70 (arrows) when it is compared with the short hairpin RNA empty vector (shControl). (D) The treatment of CQ (5 µM) or MG132 (2.5 µM) attenuates the Bmal1-mediated tau decrease as shown by an increase of tau protein levels in the presence of CQ and MG132 on western blot. EV, empty vector; FC, fold-change; sh, short hairpin.

Bmal1 regulates tau degradation via Hsp70

The disturbed circadian variation in the molecular clock, Bmal1, was evident in the tau transgenic mice. Based on that Bmal1 is a transcription factor to regulate the expression of many targets the possibility that Bmal1 controls Hsp70 and tau protein physiology was conceived. Consistent with our expectation, Hsp70 mRNA and protein levels were increased in response to the overexpression of Bmal1 in HEK293T cells (Fig. 5A). In addition, similarly to the effect of Hsp70 on tau, overexpression of Bmal1 markedly reduced the soluble and insoluble tau protein levels on western blot

following the forskolin treatment (Fig. 5B). The Bmal1-induced diminution of tau protein levels was attenuated by the knockdown of Hsp70 (shHsp70) (Fig. 5C). It suggests that the impact of Bmal1 on tau was exerted by the regulation of Hsp70 expression. To know the tau clearance machinery that was involved in Baml1-mediated tau diminution, the autophagy (CQ) and a proteasome inhibitor (MG132) were treated again while the Bmal1 expression was modulated. Both inhibitors effectively attenuated the tau degradation by Bmal1 (Fig. 5D). It shows that modulating tau clearance by Bmal1is also conducted by both autophagy and proteasome

pathways, and it supports again the idea that Bmal1 regulates tau clearance via Hsp70 (Fig. 5D).

Collectively, our results suggest that overexpression of pathological tau (P301S) in the brain could disrupt circadian oscillations. The functional shift in Bmal1 might induce the diurnal dysregulation of Hsp70 that plays a role in tau disaggregation and degradation in an autophagy and proteasome-dependent manner.

DISCUSSION

In this study, we showed an aberrant oscillation of the core molecular clock Bmal1 in the suprachiasmatic nucleus of P301S tau transgenic mice. The circadian desynchrony of Bmal1 was also evident in other brain regions, especially in the hippocampus where its rhythmic cycling was less evident in P301S mice compared to the wild-type. The functional shift of Bmal1 was continual to the diurnal dysregulation of Hsp70 and tau which demonstrated a peculiar pattern of level changes according to ZT. The circadian expression of Hsp70 revealed a similar pattern to that of the soluble tau, while the opposite to the insoluble tau. When the interactions between Bmal1 and Hsp70 in the regulations of tau status were tested *in vitro*, these were shown to increase tau degradations commonly through the autophagic and proteasomal degradation pathways. The mRNA and protein expression of Hsp70 was enhanced by Bmal1 overexpression, and the inhibition of Hsp70 expression attenuated the Bmal1-mediated tau diminution. These findings collectively suggest that the aberrant diurnal oscillations in the Bmal1 circadian clock were accompanied by distinct circadian variability in Hsp70 expression and Hsp70-associated tau disaggregation in tau transgenic mice.

The intracellular oscillations of tau protein and its solubility have never been examined in relation to the circadian clock. The impact of the circadian deficit on tau metabolism has also been described in P301S mice, as chronic sleep deprivation during early adult life accelerates the spread and aggregation of tau protein and promotes neurodegeneration and behavioral impairments [29]. And the P301L mutant human tau transgenic mice model has been examined and reported to harbor disrupted circadian rhythms accompanied by extensive tau pathology in the hypothalamus [12]. Despite studies focusing on the interrelationship between tauopathy and circadian rhythms, the underlying mechanism is not fully understood. In this study, Hsp70 is shown as a possible mediator between circadian disruption and tauopathy. The role of Hsp70 in the disassembly and degradation of tau to relieve tau accumulation has been identified and shown to oscillate in this study. The close in-phase relationship between Hsp70 and soluble tau suggests its role in tau disassembly in the tauopathy animal model. However,

the effect of Hsp70 *in vitro* on the decrease in tau was found in both the soluble and insoluble fractions. The proteostasis machinery that is impaired in P301S mice due to chronic exposure to pathologic tau could be a possible reason for these discrepancies. In this situation, the tau disaggregating effect of Hsp70 was more apparent than the degrading effect. A change in the Hsp70 level has been frequently noted in physiological and pathological conditions; however, diurnal oscillations in Hsp70 are rarely reported [30]. We cannot tell which way the aberrant oscillations of Hsp70 would work, either aggravation or prevention of tau pathology since it was not tested directly in this study. Considering its physiological function in protein disaggregation and degradation [31], it can be speculated that the aberrant oscillation of Hsp70 would further disturb the tau proteostasis in the tauopathy model. If it is correct, restoring the circadian consistency may be a strategy to reduce tau pathology. However, in drosophila Huntington's disease (HD) model the perturbance in clock function paradoxically diminished huntingtin aggregations and cellular loss [32]. Although the data was from neither mammalian nor tau pathology, it raises the necessity of further study to determine the direction of clock modulation for its potential therapeutic implications in tauopathy.

The causal relationship between disrupted oscillation of Bmal1/Hsp70 and tauopathy is not shown in this study. The aberrant diurnal oscillation of Bmal1 is thought to be induced by the unresolved accumulation of pathologic tau proteins considering that the P301S mice at the studied age demonstrate full-blown pathology [21]. Regardless of causal direction, it is very likely that there is a bidirectional relationship between circadian disruption and tauopathy [8]. We cannot exclude the possibility that another downstream target of Bmal1 exists and modulates tau status or its stability in P301S mice. Further experiments using patient-derived specimens and knockout animal models are also necessary to understand the precise regulatory processes of diurnal Hsp70 variability in tauopathy.

The current study is valuable in terms of showing the novel mechanism linking circadian disruption and tau aggregation in an animal model. We propose Hsp70 as an intermediator between tauopathy and circadian disruption. Considering that tau solubility and the expression of Hsp70 oscillated following the ZT, the precise regulation of circadian variability in these parameters could provide the solution to alleviating the accumulation of pathologic tau and restoring circadian disturbances at the same time.

ACKNOWLEDGEMENTS

REFERENCES

1. Drechsel DN, Hyman AA, Cobb MH, Kirschner MW (1992) Modulation of the dynamic instability of tubulin assembly by the microtubule-associated protein tau. Mol Biol Cell 3:1141-1154.

2. Stamer K, Vogel R, Thies E, Mandelkow E, Mandelkow EM (2002) Tau blocks traffic of organelles, neurofilaments, and APP vesicles in neurons and enhances oxidative stress. J Cell Biol 156:1051-1063.

3. Li L, Fothergill T, Hutchins BI, Dent EW, Kalil K (2014) Wnt5a evokes cortical axon outgrowth and repulsive guidance by tau mediated reorganization of dynamic microtubules. Dev Neurobiol 74:797-817.

4. Violet M, Delattre L, Tardivel M, Sultan A, Chauderlier A, Caillierez R, Talahari S, Nesslany F, Lefebvre B, Bonnefoy E, Buée L, Galas MC (2014) A major role for tau in neuronal DNA and RNA protection in vivo under physiological and hyperthermic conditions. Front Cell Neurosci 8:84.

5. Wang Y, Mandelkow E (2016) Tau in physiology and pathology. Nat Rev Neurosci 17:5-21.

6. Kent SA, Spires-Jones TL, Durrant CS (2020) The physiological roles of tau and Aβ: implications for Alzheimer's disease pathology and therapeutics. Acta Neuropathol 140:417-447.

7. Xie Y, Tang Q, Chen G, Xie M, Yu S, Zhao J, Chen L (2019) New insights into the circadian rhythm and its related diseases. Front Physiol 10:682.

8. Nassan M, Videnovic A (2022) Circadian rhythms in neurodegenerative disorders. Nat Rev Neurol 18:7-24.

9. Lucey BP, McCullough A, Landsness EC, Toedebusch CD, McLeland JS, Zaza AM, Fagan AM, McCue L, Xiong C, Morris JC, Benzinger TLS, Holtzman DM (2019) Reduced non-rapid eye movement sleep is associated with tau pathology in early Alzheimer's disease. Sci Transl Med 11:eaau6550.

10. Oh JY, Walsh CM, Ranasinghe K, Mladinov M, Pereira FL, Petersen C, Falgàs N, Yack L, Lamore T, Nasar R, Lew C, Li S, Metzler T, Coppola Q, Pandher N, Le M, Heuer HW, Heinsen H, Spina S, Seeley WW, Kramer J, Rabinovici GD, Boxer AL, Miller BL, Vossel K, Neylan TC, Grinberg LT (2022) Subcortical neuronal correlates of sleep in neurodegenerative diseases. JAMA Neurol 79:498-508.

11. Holth JK, Mahan TE, Robinson GO, Rocha A, Holtzman DM (2017) Altered sleep and EEG power in the P301S tau transgenic mouse model. Ann Clin Transl Neurol 4:180-190.

12. Stevanovic K, Yunus A, Joly-Amado A, Gordon M, Morgan D, Gulick D, Gamsby J (2017) Disruption of normal circadian clock function in a mouse model of tauopathy. Exp Neurol 294:58-67.

13. Logan RW, McClung CA (2019) Rhythms of life: circadian disruption and brain disorders across the lifespan. Nat Rev Neurosci 20:49-65.

14. Van Drunen R, Eckel-Mahan K (2021) Circadian rhythms of the hypothalamus: from function to physiology. Clocks Sleep 3:189-226.

15. Holth JK, Fritschi SK, Wang C, Pedersen NP, Cirrito JR, Mahan TE, Finn MB, Manis M, Geerling JC, Fuller PM, Lucey BP, Holtzman DM (2019) The sleep-wake cycle regulates brain interstitial fluid tau in mice and CSF tau in humans. Science 363:880-884.

16. Ishida K, Yamada K, Nishiyama R, Hashimoto T, Nishida I, Abe Y, Yasui M, Iwatsubo T (2022) Glymphatic system clears extracellular tau and protects from tau aggregation and neurodegeneration. J Exp Med 219:e20211275.

17. Xie L, Kang H, Xu Q, Chen MJ, Liao Y, Thiyagarajan M, O'Donnell J, Christensen DJ, Nicholson C, Iliff JJ, Takano T, Deane R, Nedergaard M (2013) Sleep drives metabolite clearance from the adult brain. Science 342:373-377.

18. Tang M, Harrison J, Deaton CA, Johnson GVW (2019) Tau clearance mechanisms. Adv Exp Med Biol 1184:57-68.

19. Bourdenx M, Martín-Segura A, Scrivo A, Rodriguez-Navarro JA, Kaushik S, Tasset I, Diaz A, Storm NJ, Xin Q, Juste YR, Stevenson E, Luengo E, Clement CC, Choi SJ, Krogan NJ, Mosharov EV, Santambrogio L, Grueninger F, Collin L, Swaney DL, Sulzer D, Gavathiotis E, Cuervo AM (2021) Chaperone-mediated autophagy prevents collapse of the neuronal metastable proteome. Cell 184:2696-2714.e25.

20. Suresh SN, Chakravorty A, Giridharan M, Garimella L, Manjithaya R (2020) Pharmacological tools to modulate autophagy in neurodegenerative diseases. J Mol Biol 432:2822-2842.

21. Yoshiyama Y, Higuchi M, Zhang B, Huang SM, Iwata N, Saido TC, Maeda J, Suhara T, Trojanowski JQ, Lee VM (2007) Synapse loss and microglial activation precede tangles in a P301S tauopathy mouse model. Neuron 53:337-351.

22. Lu M, Kosik KS (2001) Competition for microtubule-binding with dual expression of tau missense and splice isoforms. Mol Biol Cell 12:171-184.

23. Radziuk JM (2013) The suprachiasmatic nucleus, circadian clocks, and the liver. Diabetes 62:1017-1019.

24. Lace G, Savva GM, Forster G, de Silva R, Brayne C, Matthews FE, Barclay JJ, Dakin L, Ince PG, Wharton SB; MRC-CFAS (2009) Hippocampal tau pathology is related to neuroanatomical connections: an ageing population-based study. Brain 132(Pt 5):1324-1334.

25. Yamada K, Patel TK, Hochgräfe K, Mahan TE, Jiang H, Stewart FR, Mandelkow EM, Holtzman DM (2015) Analysis of in vivo turnover of tau in a mouse model of tauopathy. Mol Neurodegener 10:55.

26. Nachman E, Wentink AS, Madiona K, Bousset L, Katsinelos T, Allinson K, Kampinga H, McEwan WA, Jahn TR, Melki R, Mogk A, Bukau B, Nussbaum-Krammer C (2020) Disassembly of tau fibrils by the human Hsp70 disaggregation machinery generates small seeding-competent species. J Biol Chem 295:9676-9690.

27. Kawamura G, Hattori M, Takamatsu K, Tsukada T, Ninomiya Y, Benjamin I, Sassone-Corsi P, Ozawa T, Tamaru T (2018) Cooperative interaction among BMAL1, HSF1, and p53 protects mammalian cells from UV stress. Commun Biol 1:204.

28. Lim S, Haque MM, Nam G, Ryoo N, Rhim H, Kim YK (2015) Monitoring of intracellular tau aggregation regulated by OGA/OGT inhibitors. Int J Mol Sci 16:20212-20224.

29. Zhu Y, Zhan G, Fenik P, Brandes M, Bell P, Francois N, Shulman K, Veasey S (2018) Chronic sleep disruption advances the temporal progression of tauopathy in P301S mutant mice. J Neurosci 38:10255-10270.

30. Ashkenazi L, Haim A (2012) Light interference as a possible stressor altering HSP70 and its gene expression levels in brain and hepatic tissues of golden spiny mice. J Exp Biol 215(Pt 22):4034-4040.

31. Fernández-Fernández MR, Gragera M, Ochoa-Ibarrola L, Quintana-Gallardo L, Valpuesta JM (2017) Hsp70 - a master regulator in protein degradation. FEBS Lett 591:2648-2660.

32. Xu F, Kula-Eversole E, Iwanaszko M, Hutchison AL, Dinner A, Allada R (2019) Circadian clocks function in concert with heat shock organizing protein to modulate mutant huntingtin aggregation and toxicity. Cell Rep 27:59-70.e4.